EurJIC
European Journal of Inorganic Chemistry

Full Papers
doi.org/10.1002/ejic.202100168

Chemistry Europe
European Chemical Societies Publishing

Anticancer Activity and Mode of Action of Copper(II)-Bis(thiosemicarbazonato) Complexes with Pendant Nitrogen Heterocycles

Elisa Palma,[a] Paula Raposinho,*[a, b] Maria Paula Cabral Campello,[a, b] Dulce Belo,[a, b] Joana F. Guerreiro,[a] Vítor Alves,[c] Alexandra Fonseca,[c] Antero J. Abrunhosa,[c] António Paulo,[a, b] and Filipa Mendes*[a, b]

Exploring the potential of bis(thiosemicarbazones) (BTSC), a new family of BTSC ligands derived from GTSM (glyoxal-bis(N4-methylthiosemicarbazonato) and respective Cu^{II}BTSC complexes were synthesized. These complexes, having pendant nitrogen heterocycles, exhibited increased water-solubility, lower lipophilicity at physiological pH and more negative Cu(II)/Cu(I) redox potential, when compared with the parental complex. The cytotoxic evaluation performed in a panel of cancer cells lines showed an important effect of the metal complexation, and furthermore correlated well with the cellular uptake of the compounds, which was determined using their ^{64}Cu congeners. The radiolabelling of the complexes also allowed more detailed uptake studies, with the results suggesting an active transport or facilitated diffusion mechanism for the cellular uptake of **^{64}CuGTSMpip** and **^{64}CuGTSMmor**, with pendant piperidine and morpholine rings, respectively. Additionally, a comparative study with the corresponding Cu(II) complexes derived from ATSM (diacetyl-bis(N^4-methylthiosemicarbazonato) that we have previously described, demonstrated a clear difference in their lysosomotropic properties in particular for the piperidine derivatives. From this study, **CuGTSMpip** emerged as the most promising compound to be further evaluated as an anticancer metallodrug.

Introduction

The development of pharmacologically active compounds based on bis(thiosemicarbazones) (BTSC) and on their coordination to metal centers constitutes a promising field of research. BTSC, as well as their metal complexes, have received considerable attention in the design of new drugs against a range of diseases due to their broad pharmacological activity that includes antibacterial, antimalarial, antiviral and antitumoral properties.[1]

BTSC also present a strong potential for cancer theranostics, since besides their antitumoral properties, they can form complexes with different di- or trivalent metals relevant in the biomedical imaging field, such as radiometals suitable for *in vivo* clinical imaging by PET (positron emission tomography) (e.g. ^{64}Cu or ^{68}Ga) or SPECT (single-photon emission computed tomography) (e.g. ^{111}In), as well as fluorescent Zn(II) complexes for preclinical studies using optical imaging modalities.[2]

The intense research efforts on the chemistry of thiosemicarbazone (TSC) and BTSC derivatives and their metal complexes have already led to achievements with clinical translational potential. The most prominent example is the Cu(II) complex CuATSM (ATSM = diacetyl-bis(N^4-methylthiosemicarbazonato)) that, when prepared with the positron-emitting ^{64}Cu, has been successfully evaluated in patients with different tumors (e.g. lung, cervical and rectal cancers) providing useful clinical data, namely as an hypoxic-sensitive radioprobe.[3] More recently, DpC (di-2-pyridylketone 4-cyclohexyl-4-methyl-3-thiosemicarbazone) has also entered Phase 1 multi-center clinical trials as an anticancer agent to treat advanced and resistant tumors.[1c] DpC presents the ability to bind to iron and copper ions with consequent generation of intracellular reactive oxygen species (ROS) that lead to lysosomal membrane permeabilization (LMP) and cell death.[1c,4]

Taking into account the well-documented relevance of BTSC complexes with divalent metals in the biomedical field, we have recently reported the synthesis and biological evaluation of a new family of BTSC copper(II) complexes.[5] These new compounds were designed based on the functionalization of the CuATSM scaffold with pendant cyclic amines (piperidine and morpholine) introduced at the exocyclic nitrogen atoms, using appropriate methylenic linkers. The rationale behind our strategy was that the presence of the cyclic amine side chains

[a] Dr. E. Palma, Dr. P. Raposinho, Dr. M. P. C. Campello, Dr. D. Belo, Dr. J. F. Guerreiro, Dr. A. Paulo, Dr. F. Mendes
C2TN, Centro de Ciências e Tecnologias Nucleares,
Instituto Superior Técnico, Universidade de Lisboa,
Estrada Nacional 10, 2695-066 Bobadela LRS, Portugal
E-mail: paular@ctn.tecnico.ulisboa.pt
fmendes@ctn.tecnico.ulisboa.pt
[b] Dr. P. Raposinho, Dr. M. P. C. Campello, Dr. D. Belo, Dr. A. Paulo, Dr. F. Mendes
DECN, Departamento de Engenharia e Ciências Nucleares,
Instituto Superior Técnico, Universidade de Lisboa,
Estrada Nacional 10, 2695-066 Bobadela LRS, Portugal
[c] Dr. V. Alves, A. Fonseca, Dr. A. J. Abrunhosa
CIBIT/ICNAS, Instituto de Ciências Nucleares Aplicadas à Saúde,
Universidade de Coimbra,
Coimbra, Portugal

Supporting information for this article is available on the WWW under https://doi.org/10.1002/ejic.202100168

Part of the joint "Metals in Medicine" Special Collection with ChemMedChem.

could increase the water-solubility of the complexes, a crucial issue in the design of metal-based anticancer drugs, without compromising their ability to accumulate in tumoral cells and induce cytotoxic effects. Moreover, the presence of the piperidine and morpholine rings could also influence the intracellular distribution of the complexes, namely by promoting its lysosomal entrapping.[6] We have shown that piperidinyl/morpholinyl derivatives of CuATSM present a significant cytotoxic activity against a panel of human tumoral cell lines, showing a remarkably higher uptake than CuATSM in most of the tumoral cells studied. We have further evaluated how the presence of the pendant cyclic amines influences the cellular uptake, subcellular localization and the possible mechanism of action for this class of BTSC M(II) complexes, by extending the studies to fluorescent Zn(II) congeners, and followed up their cell uptake kinetics and subcellular localization by fluorescence microscopy.[7]

Although their mechanism of action is not fully understood, Cu-BTSC complexes can act as copper ionophores and their anticancer potency appears to be correlated with their ability to release coordinated copper under the reductive intracellular environment. In general, copper dissociates intracellularly from CuGTSM derivatives (GTSM = glyoxal-bis(N4-methylthiosemicarbazonato) but is retained by CuATSM derivatives, which tend to release the metal uniquely under hypoxia conditions that are present only in certain tumor cells.[8]

These differences result from the more negative Cu(II)/Cu(I) redox potential exhibited by CuATSM derivatives, when compared with the CuGTSM congeners, and certainly justify why GTSM derivatives and their Cu(II) complexes usually display a highest cytotoxicity against most common human tumoral cells.[9] Consistently, CuGTSM showed significant anticancer effects in a Transgenic Adenocarcinoma of Mouse Prostate (TRAMP) model, while CuATSM was ineffective using the same doses[9a,10] Altogether, these results indicate that GTSM compounds are more promising lead structures to develop new anticancer drugs than the ATSM counterparts. However, CuGTSM has led to significant damage to the liver and off-target renal toxicity in the reported animal studies.[9a,11] Another drawback of this class of copper complexes is their low water solubility, an issue that hindered in a few instances their preclinical evaluation as anticancer or antimicrobial agents.[12]

In this contribution, we have developed a new set of Cu^{II}BTSC complexes based on the GTSM scaffold functionalized with pendant piperidine and morpholine rings, following our previous studies with Cu-ATSM complexes functionalized with the same pendant cyclic amines.[5] We expected that the presence of these nitrogen heterocycles would lead to compounds with improved water-solubility compared with the parental CuGTSM, while maintaining its anticancer activity with reduction of unwanted side effects. In addition, we also aimed to compare the influence of the cyclic amines on the uptake and cytotoxic activity of CuGTSM and CuATSM complexes presenting a different redox behavior, which might affect the copper bioavailability in tumor cells. By using these N-heterocyclic rings, we have taken in consideration that piperidine and morpholine moieties can confer excellent water solubility to different classes of compounds, as recently demonstrated for Cu-TSC complexes.[13] In fact, both moieties are among the nitrogen heterocycle "building blocks" most commonly used to improve the solubility and/or pharmacological profile of FDA-approved small molecule drugs.[14]

To pursue this goal, we have synthesized a new family of Cu^{II}BTSC complexes derived from CuGTSM (Scheme 1) using non-radioactive copper (^{nat}Cu) and ^{64}Cu. The newly synthesized compounds were submitted to a detailed *in vitro* investigation that included: i) cyclic voltammetry experiments to characterize the redox properties of the complexes; ii) screening of the cytotoxicity for non-radioactive Cu^{II}BSTC complexes in a panel of human cancer cell lines; iii) cellular uptake experiments of the corresponding radioactive $^{64}Cu^{II}$BTSC complexes and iv) assessment of mechanisms of intracellular accumulation. For comparative purposes, CuATSM and derivatives were also evaluated in selected cellular assays.

Results and Discussion

Chemical and Radiochemical Synthesis

The new chelators synthesized in this work, **$GTSMH_2pip$** and **$GTSMH_2mor$** (Scheme 2), were obtained by an acid-catalyzed condensation reaction between glyoxal and the respective 4-substituted thiosemicarbazides (**1**–**2**), using methodologies similar to those described in the literature for related compounds.[5,15] Thiosemicarbazides **1** and **2** are relatively unstable and, for this reason, these compounds were used immediately after purification. The **$GTSMH_2pip$** and **$GTSMH_2mor$** were obtained in relatively low yield (15–17%), in part due to the difficulties encountered in their purification that required RP-HPLC in the case of **$GTSMH_2pip$**. The characterization of these GTSM derivatives was performed by ESI-MS, elemental analysis (CHN), IR spectroscopy and NMR spectroscopy (Figure S1, Figure S2 and Figure S3, and details in the experimental part). The NMR spectra of both chelators presented a splitting pattern indicating that the molecules are symmetric, and in agreement with the proposed formulations. A single signal was observed for the two NH protons adjacent to the imine groups, at downfield chemical shifts (11.78 ppm for **$GTSMH_2mor$** and 12.05 ppm for **$GTSMH_2pip$**). The NH

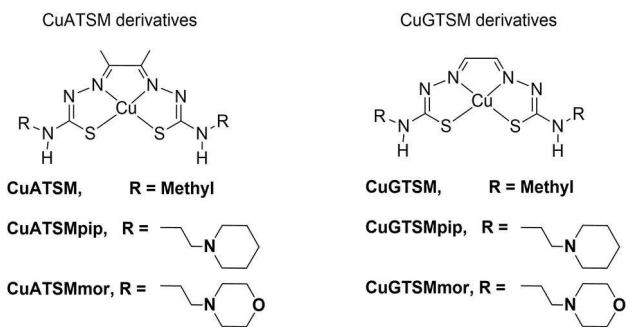

Scheme 1. Structure of CuATSM and CuGTSM and their derivatives.

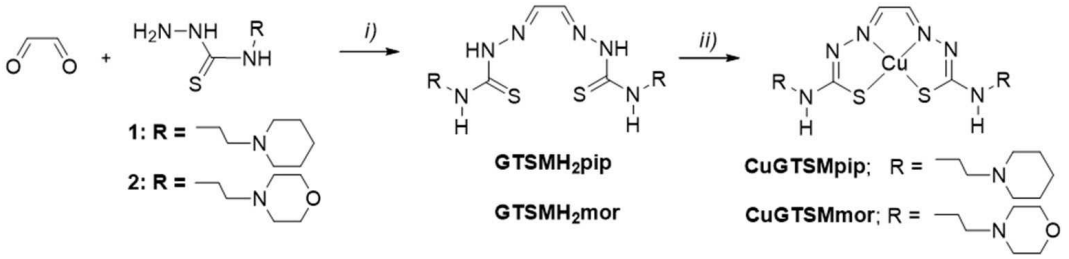

Scheme 2. Synthesis of the new BTSM chelators and respective Cu^{II} complexes (CuGTSMpip and CuGTSMmor). i) Acetic acid, ethanol, 60–70 °C; ii) $Cu(OAc)_2.2H_2O$, MeOH, R.T.

protons close to the hydrocarbonated side chains were observed as broad triplets at 8.43 and 8.72 ppm for **GTSMH$_2$mor** and **GTSMH$_2$pip**, respectively. The two imine protons (at 7.74 ppm for **GTSMH$_2$mor** and 7.77 ppm for **GTSMH$_2$pip**) originated one single singlet for each molecule. The aliphatic protons of the ethylenic chain, and piperidine and morpholine rings, gave rise to signals that resonate at chemical shifts spanning from 1.40 to 3.89 ppm.

The non-radioactive Cu^{II}BTSC complexes (**CuGTSMpip** and **CuGTSMmor**) were obtained with yields varying between 27 and 39% by reacting copper acetate with one equivalent of the corresponding ligand in methanol, as depicted in Scheme 2. These Cu(II) complexes were recovered as reddish-brown microcrystalline solids.

The characterization of **CuGTSMpip** and **CuGTSMmor** was performed by ESI-MS, elemental analysis (CHN), IR spectroscopy and RP-HPLC. The obtained analytical data are consistent with the molecular structures of these Cu(II) complexes and confirmed their high purity (Supplementary Figure S3 and details in the experimental part).

The ^{64}Cu counterparts of **CuGTSMpip** and **CuGTSMmor** were also synthesized for a more straightforward determination of the cellular uptake of the new Cu^{II}BTSC compounds in human tumoral cells. The radiochemical synthesis was done by reacting $^{64}CuCl_2$ with the corresponding ligands at room temperature, as we have previously described for related **^{64}CuATSM** derivatives.[5] All the new ^{64}Cu-BTSC complexes were obtained in almost quantitative yield (> 99%) and were stable after incubation at 37 °C in PBS and cell culture media, for at least 4 hours that corresponds to the longest time period of the biological assays.

The chemical identity of the new radioactive Cu^{II}BTSC complexes was ascertained by comparing their analytical RP-HPLC gamma-traces with the RP-HPLC UV-Vis traces of the analogues prepared with natural copper (**CuGTSMpip** and **CuGTSMmor**), as exemplified for **^{64}CuGTSMpip** in Figure 1 and in Supplementary Figure S4 and Figure S5 for **^{64}CuGTSM** and **^{64}CuGTSMmor** respectively.

The radioactive ^{64}Cu complexes were also used to assess the (lipo)hydrophilic character of the compounds. For that purpose, the partition coefficient of the complexes between n-octanol and 0.1 M PBS (pH 7.4) was determined through the measurement of the ^{64}Cu radioactivity in the organic and the aqueous phases. The respective log $D_{7.4}$ values are presented in the

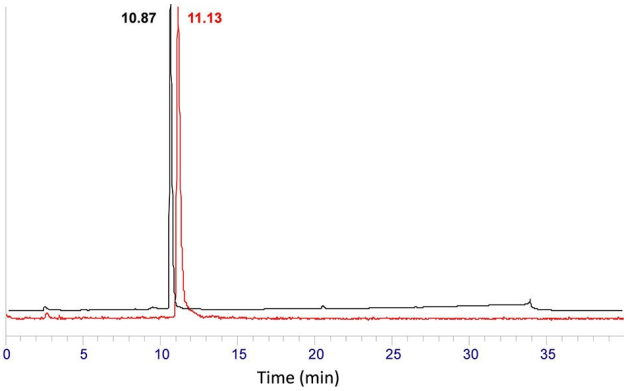

Figure 1. RP-HPLC chromatograms of $^{nat/64}$CuGTSMpip obtained using HPLC method I (UV detection in black and γ detection in red).

Experimental section (see Table 3). The new Cu^{II}BTSC complexes are less lipophilic than the parental **CuGTSM** (log $D_{7.4}$ = 1.08), at pH 7.4. Besides, the piperidine-containing complex (**CuGTSMpip**, log $D_{7.4}$ = 0.32) is less lipophilic than the morpholine -containing complex (**CuGTSMmor**, log $D_{7.4}$ = 0.89). The same trend was already obtained previously[5] for the congener **CuATSM** derivatives carrying also pendant piperidine and morpholine rings (**CuATSMpip** and **CuATSMmor**). This trend was attributed to the different protonation degree of the pendant amines, as a function of their pKa, and certainly reflects the higher basicity of the piperidine ring compared to the morpholine one.[16]

Electrochemistry

The ability of neutral bis(thiosemicarbazone)copper(II) complexes to undergo a electrochemical reduction to their monoanionic specie is an important parameter that affects their cellular retention and hypoxia selectivity. It has been reported that copper delivered by **CuGTSM** is trapped nonselectively in all cells, whereas copper delivered by **CuATSM** is retained selectively in hypoxic cells but washed out readily in normal cells.[4e] That has been attributed to the fact that **CuATSM** is more difficult to reduce than **CuGTSM**, as confirmed by us ($E^{0\prime}$ = −0.54 and −0.36 V, respectively, vs NHE). In this context, we have proceeded with the measurement of the redox potentials

of the $[Cu(II)L^{\#}]^0 \rightarrow [Cu(I)L^{\#}]^-$ reduction of complexes **CuGTSMpip** and **CuGTSMmor**, in the same way as we have previously described for the congeners **CuATSMpip** and **CuATSMmor**.[5] The redox potential of **CuGTSM**, was also determined in the same conditions, for comparative purposes. The results of these cyclic voltammetry studies, performed at room temperature in dry DMSO solutions (*vs* $Ag/AgNO_3$), are summarized in Table 1.

Our results confirmed that the effect of the substituents present on the diimine backbone governs the redox potentials of the Cu(II/I) redox couples with less influence of the alkyl substituents present at the N_4 terminal atom, as already reported in previous studies.[4e,5,18] Nevertheless, the replacement of the methyl group on the N_4-terminus of **GTSM**, by an ethyl-morpholine or an ethyl-piperidine moiety, shifts the redox potential of the $[Cu(II)L\#]^0 \rightarrow [Cu(I)L\#]^-$ process to more negative values ($\Delta E^{0\prime} = 0.10$–$0.13$ V vs NHE, respectively), meaning that **CuGTSMmor** and **CuGTSMpip** are more difficult to reduce than **CuGTSM**. We have reported earlier the same trend for the congener **CuATSM** derivatives, particularly in the case of the complexes carrying the piperidine ring.

In more detail, the complexes with an unsubstituted diimine backbone, **CuGTSM**, **CuGTSMmor** and **CuGTSMpip**, showed less negative redox potentials ($E^{0\prime} = -0.36$; -0.46 and -0.49 V vs NHE, respectively,) when compared with the corresponding dimethyl-substituted congeners, **CuATSM**, **CuATSMmor** and **CuATSMpip** ($E^{0\prime} = -0.54$, -0.55 and -0.68 V vs NHE, respectively). Furthermore, in the GTSM series the more negative reduction potential is obtained for **CuGTSMpip** ($E^{0\prime} = -0.49$ V, vs NHE) showing that this complex is a weaker oxidant than **CuGTSM**. A possible reason for this difference, as already invoked in our previous work with **CuATSM** derivatives,[5] is the formation of a more favorable intramolecular interaction, in solution, between Cu(II) and the nitrogen atom from the piperidinyl ring. Due to this interaction, there is an increase in the electronic density on the metal center and, consequently, a decrease in the reduction potential. This effect is less pronounced for **CuGTSMmor** due to the poorer coordination capability of the morpholine ring, reflecting the electron withdrawing properties of its O-atom.

Table 1. Redox potentials for the $[Cu(II)L\#]0 \rightarrow [Cu(I)L\#]$- redox process observed in the copper bis(thiosemicarbazone) complexes.

Complex	$E^{0\prime}$ ($[Cu(II)L^{\#}]^0/[Cu(I)L^{\#}]^-$) (V)[a]				
	vs. $Ag/AgNO_3$[b]	vs. NHE[c]	Relative to Fc^+/Fc couple[d]	i_{pa}/i_{pc}	E_{pa}-E_{pc}
CuGTSM	−0.86	−0.36	−0,96	1.5	0.15
CuATSM	−1,04	−0.54	−1,14[5]	1.4	0.14
CuGTSMmor	−0.95	−0.46	−1.04	1.6	0.39
CuATSMmor	−1.05	−0.55	−1.13[5]	1.6	0.27
CuGTSMpip	−0.98	−0,49	−1,07	1.6	0.25
CuATSMpip	−1.18	−0.68	−1.26[5]	1.7	0.25

[a] $E^{0\prime} = (E_{pa} + E_{pc})/2$). [b] The studies were performed under the same experimental conditions using working and counter Pt electrodes, $Ag/AgNO_3$ (10^{-3} M) as the reference electrode and DMSO as solvent. The scan rate used was 20 mV s^{-1}. [c] $E^{0\prime}$(vs. NHE) = $E^{0\prime}$(vs. $Ag/AgNO_3$) + 498 mV[17]. [d] The redox potentials were normalized relatively to the Fc/Fc^+ couple, which was used as internal reference.

Biological Evaluation on Cancer Cell Lines Cytotoxic Activity

In order to obtain insights on the antitumoral properties of the new CuGTSM derivatives, their cytotoxic activities were studied in a panel of human tumoral cell lines and compared with those of the respective chelators and with the parental complex **CuGTSM**. For these assays, cells were incubated with increasing concentrations of the compounds for 48 h at 37 °C, and the cellular viability was evaluated by the MTT assay. The inhibition of growth (%) was calculated and the IC_{50} were determined and are presented in Table 2.

Among the new Cu^{II}GTSM complexes, **CuGTSMpip**, contrarily to **CuGTSMmor**, exhibited sub-micromolar IC_{50} values against all cancer cell lines, ranging between 0.05 and 0.3 μM, which is indicative of a pronounced cytotoxicity. For the majority of the cell lines evaluated, the cytotoxicity of **CuGTSMpip** was very similar to the one attained for **CuGTSM**. These values can be considered comparable or even better than those reported by other authors for the activity of **CuGTSM** in other human tumoral cell lines.[4e]

The IC_{50} values measured for **CuGTSMmor** are in the range 0.35–4.15 μM and are 8–23 fold higher than those determined for **CuGTSMpip**, depending on the cell lines tested. These data show that **CuGTSMpip** is considerably more cytotoxic than **CuGTSMmor**. Surprisingly, the cytotoxicity of **CuGTSMmor** (IC_{50} values = 0.58–1.13 μM) is almost identical or slightly lower than the one that we have determined previously for the ATSM counterpart, **CuATSMmor** (IC_{50} values = 0.72 μM), in MCF-7 cells. This trend is quite different from that previously reported by other authors for the parental **CuGTSM** and **CuATSM** pair, being **CuGTSM** a significantly more cytotoxic compound as mentioned above.[4e,9a] In our hands, the IC_{50} value obtained for **CuGTSM** in MCF-7 cells was 0.01 μM while the same value for **CuATSM** was 0.74 μM, respectively.[5] The same trend was

Table 2. IC_{50} (μM) values of the Cu^{II}GTSM derivatives and respective ligands in human tumoral cell lines: breast carcinoma (MCF-7), glioblastoma (U87), and prostate carcinoma (LNCAP and PC3).

	IC_{50} [μM]			
	MCF-7	U87	LNCAP	PC3
$GTSMH_2$	0.2 ± 0.05	8.60 ± 2.95	0.144 ± 0.09	14.10 ± 5.51
$GTSMH_2$mor	5.74 ± 2.90	10.40 ± 6.47	0.49 ± 0.27	11.82 ± 6.08
$GTSMH_2$pip	1.03 ± 0.45	6.99 ± 3.45	0.13 ± 0.04	7.02 ± 2.82
CuGTSM	0.01 ± 0.002	0.38 ± 0.09	0.1 ± 0.02	0.31 ± 0.14
CuGTSMmor	1.13 ± 0.25	4.11 ± 0.06	0.58 ± 0.11	4.15 ± 1.19
CuGTSMpip	0.05 ± 0.001	0.29 ± 0.06	0.07 ± 0.02	0.21 ± 0.03

observed for **CuGTSMpip** and **CuATSMpip** in the MCF-7 cell line with IC_{50} values of 0.05 and 0.27 μM.

As observed previously for the corresponding CuATSM derivatives,[5] there was a clear effect of metal-complexation on the cytotoxic profile of the compounds as the Cu(II) complexes are much more cytotoxic than the corresponding ligands. For instance, for PC3 cells that showed the highest increase in cytotoxicity with metal-complexation, the IC_{50} value for **GTSMpip** is about 7 μM, while the respective Cu-complex presented a value 32 times lower (0.21 ± 0.03 μM).

Time- and Temperature-Dependent Cellular Uptake

To understand how the accumulation of the newly synthesized Cu^{II}GTSM derivatives in tumoral cells would influence their cytotoxic activity, the uptake of the radiolabeled complexes (**^{64}CuGTSM, ^{64}CuGTSMmor** and **^{64}CuGTSMpip**) was evaluated by quantitative gamma-counting measurements in PC3 human prostate cancer cells at 37 °C, for up to 4 h. The results are represented in Figure 2.

These studies revealed an important and time-dependent cellular uptake at 37 °C for all ^{64}Cu-complexes (Figure 2a). The uptake curve of **^{64}CuGTSMpip** in PC3 cells had the highest slope for short incubation times; this complex also showed the highest uptake value, reached after 3 h of incubation (469 ± 18 % as a percentage of total activity applied, per million cells). The plateau values of the cellular uptake curves varied in the order **^{64}CuGTSMpip** > **^{64}CuGTSM** > **^{64}CuGTSMmor** being observed a much lower uptake for **^{64}CuGTSMmor** (< 150 % as a percentage of total activity applied, per million cells). Interestingly, all the ^{64}CuGTSM derivatives presented higher cellular uptakes than the corresponding ^{64}CuATSM derivatives that we have described.[5] To examine whether the accumulation of the ^{64}Cu-complexes (both for the ATSM and GTSM derivatives) occurs through active or passive processes, a temperature-dependent analysis of the cellular uptake was performed. Active carrier-mediated transport or facilitated diffusion are expected to be inhibited at low temperature, while passive uptake should remain unaffected under low-temperature conditions.

To assess the influence of temperature on the cellular uptake, PC3 cells were exposed to **^{64}CuATSM** and **^{64}CuGTSM** derivatives at 37 °C or 4 °C, for different periods, up to 4 h. The results are shown in Figure 2b and Figure 2c with the uptake values presented as percentage by million cells.

The cellular uptake of **^{64}CuGTSMpip** and **^{64}CuGTSMmor** was extensively inhibited at 4 °C compared to 37 °C. For instance, at 2 h of incubation, the uptake values of **^{64}CuGTSMpip** decreased from 452 to 32 % (Figure 2b), which corresponds to a reduction of more than 90 %. This strongly temperature-dependent uptake is consistent with the predominance of an active transport mechanism or facilitated diffusion for the uptake of the CuGTSM complexes carrying the nitrogen heterocycles. In contrast, a small temperature-dependent effect was observed for the **^{64}CuGTSM** accumulation in PC3 cells (Figure 2b). Indeed, the uptake curves of **^{64}CuGTSM** at 4 °C and 37 °C were parallel, presenting an uptake inhibition of about 50 % at 2 h (from 337

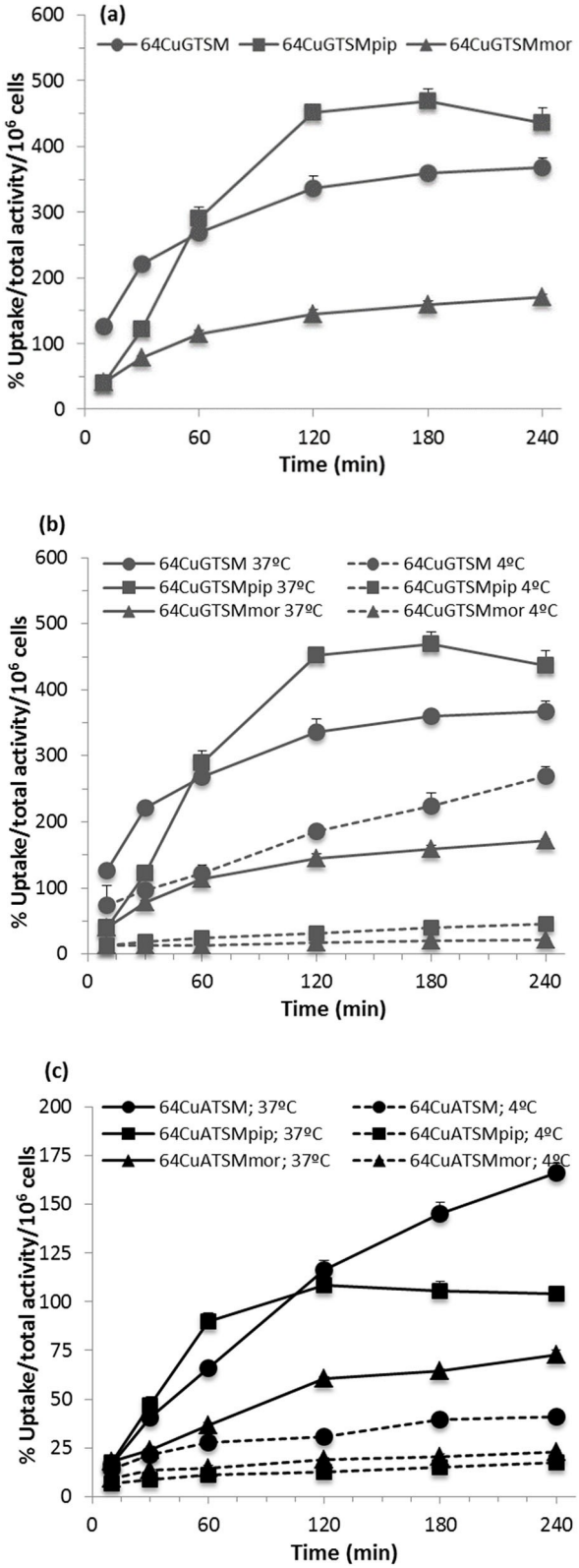

Figure 2. Uptake of **^{64}CuGTSM** derivatives in PC3 cells: (a) Cellular uptake of **^{64}CuGTSM** derivatives in PC3 cells at 37 °C, during a 4 h period. Effect of the temperature on the cellular uptake of ^{64}Cu-complexes in prostate carcinoma PC3 cells (incubation at 4 °C and 37 °C, during a 4 h period): (b) **^{64}CuGTSM** derivatives and (c) **^{64}CuATSM** derivatives. Activity associated with the cell (cellular uptake) expressed as a percentage of total activity applied, and per million cells. Results were calculated from independent biological replicates (n = 4), and are given as the average ± SEM.

to 187%). These results indicate that an active mechanism is not predominant in the uptake of **^{64}CuGTSM**, with a passive mechanism likely being more relevant in this case.

The cellular uptake of the **^{64}CuATSM** derivatives was significantly inhibited at 4 °C when compared to the one obtained at 37 °C, including for the parental **^{64}CuATSM** (Figure 2c). Upon lowering the temperature, the following inhibition of the cellular uptake values was observed for these ^{64}Cu-complexes at 2 h of incubation: **^{64}CuATSM**, from 116 to 31% (ca. 80% reduction); **^{64}CuATSMpip**, from 108 to 13% (ca. 90% reduction); **^{64}CuATSMmor**: from 61 to 19% (ca. 70% reduction). This temperature-dependent activity is consistent with a role for active or facilitated transport mechanisms in the uptake of all these **^{64}CuATSM** derivatives in the PC3 cell line. However, some differences were found in their kinetic uptake profiles, suggesting the involvement of diverse mechanisms. Among all the tested radiocomplexes, **^{64}CuATSMmor** presented the lowest uptake in PC3 cells for all the tested time points. The time-dependent uptake of **^{64}CuATSMpip** had a different kinetics when compared with **^{64}CuATSM**. Namely, the cellular accumulation of **^{64}CuATSMpip** was faster and reached its highest value after 2 h of incubation; **^{64}CuATSM** exhibited an initial slower uptake kinetics but a steadily increasing uptake throughout the duration of the assay, surpassing that of **^{64}CuATSMpip** after about 2 h of incubation.

In summary, the time- and temperature-dependent cellular assays have shown that all the **^{64}CuGTSM** derivatives present a higher uptake in PC3 cells than the **^{64}CuATSM** counterparts. Most probably, this reflects the easiest ability of **CuGTSM** derivatives to be reduced intracellularly under normoxia conditions. Excepting **^{64}CuGTSM**, the important effect of temperature on the cellular uptake indicates the involvement of active carrier-mediated transport. Recently, the same type of effect has been reported for Cu-TSC complexes functionalized with pendant morpholine groups.[13] The planarity, lipophilicity and smaller size of **^{64}CuGTSM** certainly enable a more facile passive diffusion through the lipid bilayer. However, for each of the complexes we cannot exclude the simultaneous occurrence of carrier-facilitated diffusion and passive diffusion, as often encountered for small molecule drugs.[19]

For the Cu-GTSM derivatives, the cytotoxicity of the cold compounds varied in the order **CuGTSM≅CuGTSMpip > CuGTSMmor** and is proportional to the cellular uptake of the ^{64}Cu congeners but not to the respective lipophilicity at physiological pH. At pH 7.4**, CuGTSMmor** is more lipophilic (log $D_{7.4} = 0.89$) than **CuGTSMpip** (log $D_{7.4} = 0.32$), which certainly reflects the different ionization degrees of the compounds, as discussed above. For this reason, the measured lipophilicity does not reflect directly the capability of the complexes to cross the cell membrane, which is expected to be higher for the neutral forms that will more probably be the dominant species crossing the cell membrane. In this respect, the neutral **CuGTSMpip** is expected to be more lipophilic than the neutral **CuGTSMmor** that contains more polar oxygen atoms in the N-heterocyclic rings. All in all, the biological data indicate that these **Cu-GTSM** complexes act as copper ionophores with an anticancer activity that is well-correlated with their ability to accumulate in tumor cells and, eventually, to release coordinated copper under the reductive intracellular environment.

Evaluation of the Uptake via Sigma-1 Receptor

Considering the indication of a possible active or facilitated mechanism of uptake and also the observation in the literature that radiolabelled piperidines can act as sigma-1 receptor ligands,[20] we decided to test the hypothesis that our ^{64}Cu-complexes could enter the cells through a mechanism involving the σ1 receptors (σ1R). This study comprised cellular uptake assays of the **^{64}Cu-GTSM** derivatives in the presence of a σ1 receptor inhibitor, haloperidol, using tumoral cells lines with different levels of expression of σ receptors.[21] Therefore, uptake-blocking studies were performed for **^{64}CuGTSM**, **^{64}CuGTSMpip** and **^{64}CuGTSMmor**, using haloperidol (10 μM concentration) in the human prostate cancer cell lines PC3 and DU145, with the latter presenting a higher σ1 receptors density than the former.[21]

Firstly, higher levels of uptake for **^{64}CuGTSM** and **^{64}CuGTSMpip** were not observed in DU145 cells comparatively with PC3 cells, indicating that σ1 receptors might not be involved in their mechanism of uptake (see Supplementary Figure S14). Only the complex with the lowest values of uptake, **^{64}CuGTSMmor**, presented higher uptake in DU145 than in PC3 cells. Furthermore, blocking studies performed with haloperidol revealed no reduction of the uptake for any of the ^{64}Cu-complexes tested in the presence of the σ1R-inhibitor, either in PC3 and DU145 cells (see Figure S14). These results seem to corroborate that σ1 receptors do not mediate the uptake of the complexes under study.

Cellular Retention

Following the temperature-dependency studies, we performed efflux experiments in PC3 cells for **^{64}CuATSMpip** and **^{64}CuATSMmor**, and for **^{64}CuGTSMpip** and **^{64}CuGTSMmor**, in comparison with the parental complexes **^{64}CuATSM** and **^{64}CuGTSM**, in order to understand how the presence of the pendant cyclic amines affected the intracellular retention of the Cu^{II}BTSC complexes. Cells were incubated with the ^{64}Cu-complexes for 2 h 30 at 37 °C to allow the cellular uptake to occur, after which they were washed and re-incubated with culture medium to determine the efflux during a 24 h time period. The cellular retention of the complexes, expressed in percentage of total initial uptake, is presented in Figure 3.

A slow washout was observed for all complexes in the PC3 cell line, with cells showing more than 50% of internalized activity after 4 h. Noticeably, the cellular retention pattern of **^{64}CuGTSMpip** and **^{64}CuGTSMmor** was almost coincident with that exhibited by **^{64}CuGTSM** and a similar trend was observed for the **^{64}CuATSM** derivatives. These results indicate that the presence of the pendant cyclic amines does not influence their cellular efflux even if they might have a role in the mechanism of entrance of these compounds into the cells.

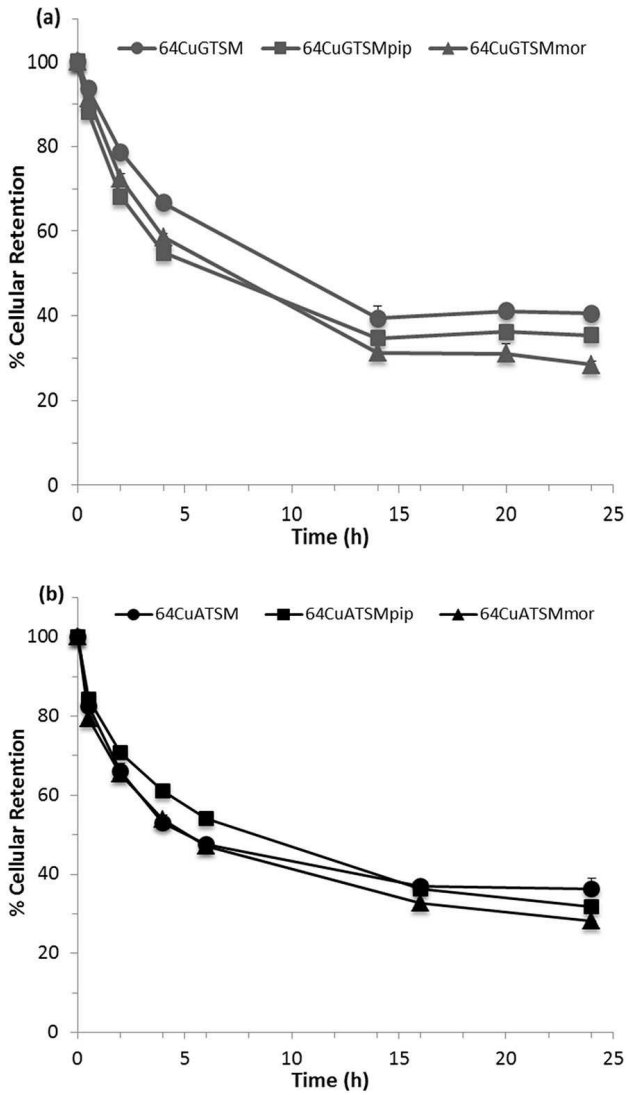

Figure 3. Cellular efflux of ^{64}Cu-complexes in PC3 prostate carcinoma cells. (a) **^{64}CuGTSM** derivatives. (b) **^{64}CuATSM** derivatives. Results were calculated from independent biological replicates (n = 4), and are given as the average ± SEM.

Evaluation of Lysosomal Accumulation

It is well described in the literature that weak bases can become trapped in cells via sequestration in intracellular acidic organelles, primarily in lysosomes but also in endocytic compartments.[22] Weak bases with pKa values greater than 7.0 can readily diffuse as neutral molecules across membranes into the cells and then into acidic lysosomes (pH ~ 5.5), where the basic moiety becomes protonated. As increasing amounts of weak base accumulate in the lysosomes, the free proton pool is depleted and consequently, the lysosomal pH increases and sequestration of the drug within lysosomes reaches saturation.[23]

To test the hypothesis that ^{64}Cu-complexes could be trapped as a protonated weak base within lysosomes, due to the presence of the protonable pendant cyclic amine groups,[6b,24] we measured the uptake of selected radiocomplexes in PC3 cells pretreated during 30 min with a competing agent, tamoxifen. Tamoxifen is a weak base (pKa of 8.5) that is able to accumulate within those organelles and raise the pH as a consequence. The effect of tamoxifen, at 10^{-4} M concentration, on the cellular uptake of the radiocomplexes selected for this study (**^{64}CuGTSM** and **^{64}CuGTSMpip**; **^{64}CuATSM** and **^{64}CuATSMpip**) is presented in Figure 4. The effect of different tamoxifen concentrations (10^{-6}–10^{-4} M) on their cellular uptake is shown in Supplementary Figure S15.

We found that pre-blocking with the tamoxifen inhibitor even at the highest concentration of 10^{-4} M did not affect the uptakes of **^{64}CuGTSM** (Figure S15a), **^{64}CuGTSMpip** (Figure S15b) and **^{64}CuATSM** (Figure S15c). In contrast, pre-incubation with tamoxifen (10^{-4} M) reduced, albeit modestly, the accumulation of **^{64}CuATSMpip** in PC3 cells by ~15 to 20% (Figure 4 and Figure S15d), suggesting that this complex can accumulate within lysosomes.

Since the results obtained in the uptake assay with the tamoxifen inhibitor suggested a potential lysosomal trapping of **^{64}CuATSMpip**, we tried to obtain further indications that would support this conclusion. For this purpose, we assessed whether pre-incubation with the cold Cu(II) compounds would lead to an altered cellular accumulation of a lysosomotropic weak base, the red-fluorescent dye LysoTracker Red.[25] If significantly accumulated in the lysosomes, the Cu(II) complexes carrying the weak basic N-heterocycles should increase the pH of this organelle with consequent reduction of the incoming fluorescent dye. The results indeed show a clear decrease in lysosomal staining in cells pre-incubated with **CuATSMpip** but not with any of the other compounds (Figure 5), which further suggests that **CuATSMpip** might become trapped in the lysosome of PC3 cells.

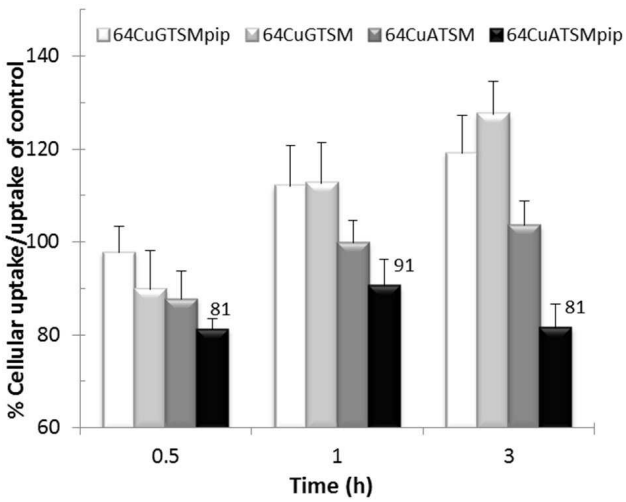

Figure 4. Effect of tamoxifen on the cellular uptake of **^{64}CuGTSM**, **^{64}CuGTSMpip**, **^{64}CuATSM** and **^{64}CuATSMpip** in prostate carcinoma PC3 cells, at 37 °C. Cellular uptake expressed as a percentage of uptake control without tamoxifen. Results were calculated from independent biological replicates (n = 4), and are given as the average ± SEM.

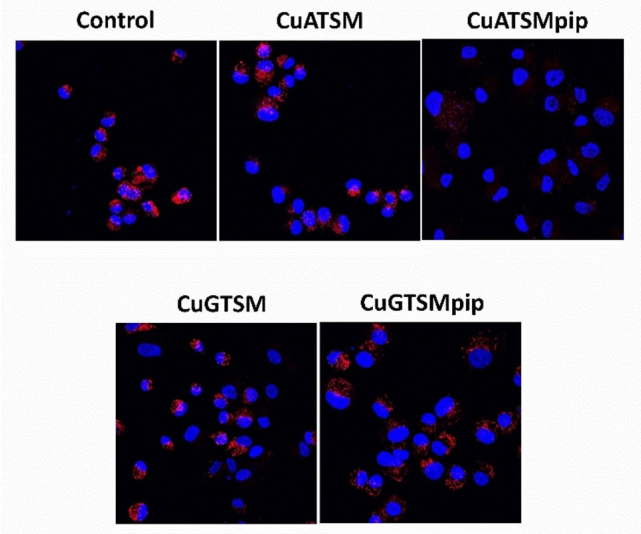

Figure 5. Effect of the pre-incubation with cold Cu-complexes in the accumulation of LysoTracker Red in cellular lysosomes of prostate carcinoma PC3 cells. Cells were visualized using confocal microscopy. The images shown are representative of one independent biological replicate.

The lysosomotropic behavior observed for **CuATSMpip** is in clear contrast with the other complexes, certainly due to structural and electronic factors. The presence of the nitrogen heterocycle justifies the difference with the parental **CuATSM** and **CuGTSM**, which do not carry a pendant protonable weak base to promote its lysosomal entrapment. On the other side, **CuGTSMpip** is expected to be reduced intracellularly more easily than **CuATSMpip**. The reduction of Cu(II) is accompanied by the release of the **GTSMH$_2$pip** ligand that can undergo deprotonation at the thiosemicarbazone functions, being eventually less prone to reach the lysosomes when compared with the original neutral Cu(II) complex.

Conclusion

We have shown that the functionalization of Cu^{II}-GTSM and Cu^{II}-ATSM complexes with pendant cyclic amines influences their mechanisms of cellular uptake and anticancer activity, this being more noticeable for the Cu^{II}-GTSM complexes for which we observed a strong influence of the pendant amine (piperidine versus morpholine) in their cytotoxic potency.

CuGTSMpip retained the cytotoxic potency of **CuGTSM** in a panel of human tumor cells, while **CuGTSMmor** is significantly less active (11 to 41-fold increase of IC_{50} values) in all tested cell lines. The cytotoxic potency is well correlated with the cellular uptake of the compounds, which was determined using the ^{64}Cu congeners. These results are in contrast with those that we have reported previously for the correspondent copper ATSM complexes (**CuATSM**, **CuATSMpip** and **CuATSMmor**), which display similar cytotoxic activity independently of the presence and nature of the pendant cyclic amine.

The cellular studies performed showed that the uptake of **CuGTSM** involves mainly a passive mechanism, unlike its derivatives carrying the nitrogen heterocycles, **CuGTSMpip** and **CuGTSMmor**, which are uptaken by the cells predominantly by active transport or facilitated diffusion mechanisms. In contrast to **CuGTSM**, **CuATSM** presented an important contribution of active processes in its cellular uptake. The active transport mechanisms appear also to be dominant in the cellular uptake of **CuATSMpip** and **CuGTSMmor**.

The induction of lysosomotropic properties by the presence of the piperidine group in **CuATSMpip** but not in **CuGTSMpip** is another striking difference between the biological behavior of the CuGTSM and CuATSM complexes studied in this work. Most probably, this difference reflects the less negative Cu(II)/Cu(I) redox potential of **CuGTSMpip** that facilitates its intracellular reduction and consequent release of the BTSC chelator carrying the lysosomotropic group.

In summary, **CuGTSMpip** showed a cytotoxic activity very similar to that of the parental **CuGTSM** and emerged as the most promising compound to be further evaluated as an anticancer metallodrug. This is already foreseen and should include studies in tumor-bearing mice to assess treatment efficacy and verify if **CuGTSMpip** can minimize the side-effects reported for **CuGTSM**, such as liver and renal toxicity. At physiological pH, **CuGTSMpip** is less lipophilic than **CuGTSM** and, therefore, might have a lower accumulation and faster clearance from off-target organs (e.g., kidney or liver) with possible reduction of side effects.

Experimental Section

General reagents and methods

All chemicals were p.a. grade and were used without purifications unless stated otherwise. The complexes CuATSM and CuGTSM were synthesized as described in the literature.[4e,15,26]

The synthesis of the 4-*N*-substituted 3-thiosemicarbazides (4-(2-(piperidin-1-yl)ethyl)-3-thiosemicarbazide (**1**) and 4-(2-(morpholin-1-yl)ethyl)-3-thiosemicarbazide (**2**)) and CuATSM derivatives (**CuATSMpip** and **CuATSMmor**) was done as described previously.[5] The chemical reactions were followed by TLC. ^{1}H and ^{13}C NMR spectra were recorded on a Varian Unity 300 MHz or 400 MHz spectrometer at the frequencies of 300 or 400 MHz (^{1}H) and 75 or 100 MHz (^{13}C), respectively. ^{1}H and ^{13}C chemical shifts (δ) are reported in ppm relative to residual solvent signals (DMSO-d_6: 2.50 ppm for ^{1}H NMR, 39.52 for ^{13}C NMR). Electrospray ionization mass spectrometry (ESI-MS) was performed on a QITMS instrument in positive and negative ionization mode. Elemental analyses were recorded on an EA 110CE automated instrument. IR spectra were recorded in KBr pellets on a Bruker Tensor 27 spectrometer.

Reversed-phase high performance liquid chromatography (RP-HPLC) analyses of natural and radioactive copper complexes were performed with a Perkin Elmer LC pump 200 coupled to a LC 290 tunable UV-vis detector and to a Berthold LB-507 A radiometric detector. For HPLC analysis with method I (flow = 1 mL/min), a Macherey-Nagel C18 reversed-phase column (Nucleosil 5 mm, 250 × 4 mm) was used; for HPLC purification with method II (flow = 2 mL/min), a semi-preparative Supelco Discovery ® BioWide Pore C18 reversed-phase column (25 cm × 10 mm × 10 μm) was used. HPLC

solvents consisted of 0.1% CF_3COOH in H_2O (solvent A) and 0.1% CF_3COOH solution in acetonitrile (solvent B).

Method I (gradient): t = 0–25 min, 90–10% eluent A; 25–27 min, 10–0% eluent A; 27–30 min, 0% eluent A; 30–32 min, 0–90% eluent A; 32–40 min, 90% eluent A.

Method II (gradient): t = 0–25 min, 90–75% eluent A; 25–30 min, 75–0% eluent A; 30–32 min, 0% eluent A; 32–35 min, 0–90% eluent A; 35–40 min, 90% eluent A.

General procedure for the synthesis of GTSM derivatives

The 4-N-substituted-3-thiosemicarbazides 1 or 2 (ca. 6 mmol, 2.5 equiv.) were dissolved in 4 mL of ethanol, and then glyoxal (1 equiv.) and 6 drops of acetic acid were added dropwise. The reaction mixture was stirred overnight at 70–80 °C. The work-up used to obtain the desired compounds (**$GTSMH_2$mor** and **$GTSMH_2$pip**) is described below, together with their characterization.

$GTSMH_2$pip: After cooling the reaction mixture till room temperature, a bright yellow solid was isolated and washed with ethanol (2×10 mL) and water (2×10 mL). After RP-HPLC purification (Method II), the title compound was obtained as a microcrystalline solid after removal of the solvents and drying under vacuum. Yield: 15%. ES + MS in H_2O/ACN for $C_{18}H_{34}N_8S_2$ (426.23), m/z: 427.7 $[M+H]^+$; ^{1}H NMR (DMSO-d_6, 300 MHz) δ: 1.40 (m, 4H), 1.66 (m, 8H), 1.79 (m, 4H), 2.92 (m, 4H), 3.25 (m, 2H), 3.89 (m, 6H), 7.77 (s, 2H, CH), 8.72 (br t, 2H, NH), 12.05 (s, 2H, NH); ^{13}C NMR (DMSO-d_6, 75 MHz) δ: 24.14 (pip), 25.74 (pip), 40.80, 53.97 (pip), 57.95, 140.31 (C=N), 176.72 (NHC=S). Anal. calcd. for $C_{18}H_{34}N_8S_2.3\ CF_3COOH.1.5\ H_2O$: C 36.22, H 5.07, N 14.08; found: C 36.18, H 5.04, N 14.08%; IR (KBr, ν/cm^{-1}): 3134.73 (m, N–H), 2934.39 (s), 1515.35 (vs, C=N), 1505.75 (vs, C=N), 1208.95 (s, thioamide), 1115.40 (s, N–N), 924.98 (w), 754.55 (w).

$GTSMH_2$mor: After cooling to room temperature, triethylamine was added until basic pH (ca. 8–9). The aqueous phase was diluted with water (50 mL) and extracted with dichloromethane (2×50 mL). The organic phase was dried over Na_2SO_4, filtered and concentrated to give a yellowish solid, which was washed with dichloromethane and n-hexane. Yield: 17%. ES + MS in DMSO/ACN for $C_{16}H_{30}N_8O_2S_2$ (430.19), m/z: 431.8 $[M+H]^+$; ^{1}H NMR (DMSO-d_6, 300 MHz) δ: 2.40 (m, 10H), 3.57 (m, 12H), 7.74 (s, 2H, CH), 8.43 (t, 2H, J = 3.0 Hz, NH), 11.78 (s, 2H, NH) (two proton signals are under the residual peak of DMSO, as demonstrated by g-HSQC NMR spectroscopy); ^{13}C NMR (DMSO-d_6, 75 MHz) δ: 53.18 (morpholine), 56.36, 66.30 (morpholine), 140.25 (C=N), 176.70 (NHC=S) (two carbon signals (2×$\underline{C}H_2$) are under the residual peak of DMSO, as demonstrated by g-HSQC NMR spectroscopy). Anal. calcd. for $C_{16}H_{30}N_8S_2O_2$.EtOH: C 45.35, H 7.61, N 23.51; found: C 46.09, H 7.67, N 23.35%; IR (KBr, ν/cm^{-1}): 3249.20 (m, N–H), 2944.92, 1529.30 (vs, C=N), 1505.75 (vs, C=N), 1199.89 (s, thioamide), 1116.21 (s, N–N), 937.65 (w), 611.68 (w).

General procedure for the synthesis of bis (thiosemicarbazonato) copper (II) complexes

To a suspension of the bis(thiosemicarbazone) ligand (0.1 mmol) in 3 mL of methanol was added a methanolic solution of one equivalent of copper acetate monohydrate (2 mL), and the mixture was stirred under RT overnight. To obtain **CuGTSMmor** and CuGTSMpip the reaction solvent was concentrated to ~3 mL and diethyl ether was added. The complexes precipitated after overnight standing at 4 °C, as dark red-brown solids.

CuGTSMpip: Yield: 27%. ES + MS in MeOH for $C_{18}H_{32}CuN_8S_2$ (487.15), m/z: 488.5 $[M+H]^+$; Anal. calcd. for $C_{16}H_{28}CuN_8O_2S_2.CH_3OH$: C 43.87, H 6.98, N 21.54; found: C 43.66, H 6.64, N 21.40%; IR (KBr, ν/cm^{-1}): 3404.83 (m, N–H), 2942.18 (m), 1534.19 (vs, C=N), 1384.35 (sharp, s), 1252.39 (s, thioamide), 1123.23 (s, N–N), 756.04, 617.53.

CuGTSMmor: Yield: 39%. ES + MS in DMSO/ACN for $C_{16}H_{28}CuN_8O_2S_2$ (491.11), m/z: 492.1 $[M+H]^+$; Anal. calcd. for $C_{16}H_{28}CuN_8O_2S_2.3H_2O$: C 35.19, H 6.27, N 20.52; found: C 35.11, H 5.82, N 20.20%; IR (KBr, ν/cm^{-1}): 3421.54 (vs broad, N–H), 2957.43 (w), 2359.98 (s), 1521.90 (vs, C=N), 1271.28 (vs, thioamide), 1113.81 (vs, N–N), 924.12 (w), 668.69 (w).

Cyclic voltammetry

Cyclic voltammetry data were obtained using a BAS C3 Cell Stand. The voltammograms were recorded at room temperature, with a scan rate of 100 mV/s, using Pt wire working and counter electrodes and an $Ag/AgNO_3$ (10^{-3} M, acetonitrile solution) reference electrode. The measurements were performed on fresh DMSO solutions with a concentration of 10^{-3} M of the analyte and 10^{-1} M of tetrabutylammonium hexafluorophoshate (*n*-Bu_4PF_6) as the supporting electrolyte. Ferrocene was added directly to the solution after analysis of the analyte of interest to allow the potentials normalization, in situ, relatively to the ferrocene/ferrocenium couple redox potential. The $E^{0\prime}$ ($[CuL^{\#}]^0 \rightarrow [CuL^{\#}]^-$) values are reported as the mid-point between the anodic (Epa) and cathodic (Epc) peaks, $E^{0\prime} = (E_{pa} + E_{pc})/_2$.

General procedure for the synthesis and characterization of the radioactive ^{64}Cu complexes

Copper-64 was produced by the ^{64}Ni(p,n)^{64}Cu nuclear reaction in a IBA Cyclone 18/9 cyclotron and supplied as $^{64}CuCl_2$(aq) in 0.1 M HCl. The radiocopper complexes were synthesized according to previously described methods.[5] Briefly, 150 μL of $^{64}CuCl_2$ in 0.1 M HCl were buffered with 200 μl of 3 M sodium acetate, followed by addition of 100 μL of a solution of ligand in DMSO (at 1 mg.mL^{-1}) and the reaction mixture was vortexed for 1 min. The resultant solution was left to react at RT for 1–2 minutes, and the labeling efficiency was determined by radio-HPLC using the conditions described above. The complexes were further purified by using a Sep-Pak C18 cartridge, essentially to remove excess DMSO. The cartridge was pre-conditioned with 2 mL of ethanol and 5 mL of distilled water and the reaction mixtures were applied to the cartridge; the cartridge was washed with ca. 7 ml of water and then, the radiocomplexes were recovered with 0.2–0.4 mL of ethanol. The ethanolic fraction was concentrated to dryness under nitrogen flux and dissolved in 100 μL of phosphate-buffered saline (PBS) solution to be used in biological assays.

The radiochemical purity of the recovered ^{64}Cu-complexes was determined by radio-HPLC (Method I), as described above, together with thin-layer chromatography (TLC) on silica gel plates (Merck 60 F254, Merck, USA) using 10% ammonia in methanolic solution. TLC plates were analyzed using a miniGita Star software from Raytest (Straubenhardt, Germany): Rf ca. 0 for ^{64}Cu-acetate and $^{64}CuCl_2$ and Rf ca. 0.65 to 0.80 for the ^{64}Cu complexes with the GTSM and ATSM ligands (Supplementary Figures S6–S10) All the radiocomplexes were obtained with a radiochemical purity > 99%.

Lipophilicity determination

The lipophilicity of the radiocomplexes was evaluated by the "shake-flask" method.[27] Briefly, the radioactive complexes were added to a mixture of octanol (1 mL) and 0.1 M PBS pH 7.4 (1 mL),

previously saturated in each other. This mixture was vortexed and centrifuged (3000 rpm, 10 min, RT) to allow phase separation. Four aliquots of both octanol and PBS were counted in a gamma counter. The octanol-water partition coefficients were calculated by dividing the counts in the octanol phase by those in the buffer. The results expressed as log $D_{7.4}$ are presented in Table 3.

Stability studies

Stability studies of ^{64}Cu complexes were performed in the presence of PBS 7.4 buffer solution or cell culture media (DMEM). These solutions were added to the purified labeled compound to afford a final dilution of 1:10. The activity used for each essay was around 35 to 40 μCi. The compounds were incubated at 37 °C for 30 min, 1 h and 4 h. ^{64}Cu complexes in the presence of PBS were analyzed by RP-HPLC and TLC radiochromatography, and the ones in the presence of DMEM were analyzed by TLC radiochromatography. As an example, we present in the SI the results obtained for **^{64}CuGTSMpip**, which were extended until 24 h (Supplementary Figures S11–S13).

Cell culture

Human prostate cancer cell lines PC3 (ECACC 90112714), LNCAP and DU145 (kindly provided by the Portuguese Institute of Oncology-Porto, Portugal) were maintained in RPMI 1640 Medium. MCF7 breast carcinoma cells (ATCC HTB-22) and U87 MG glioblastoma cells (ATCC HTB-14) were grown in DMEM containing GlutaMax and MEM, respectively. The culture media were supplemented with 10% heat-inactivated fetal bovine serum (FBS). All culture media and supplements were from Gibco, Invitrogen, UK. Cells were cultured in a humidified atmosphere of 95% air and 5% CO_2 at 37 °C (Heraeus, Germany) and tested for mycoplasma using the LookOut® mycoplasma PCR Detection kit.

Cytotoxicity evaluation

The cytotoxicity of the BTSC chelators and corresponding Cu(II) complexes was assessed by evaluating their effects on cellular proliferation using the [1-(4,5-dimethylthiazol-2-yl)-2,5-diphenyl tetrazolium] (MTT) assay. Cells were seeded in 96-well culture plates at a density of 1.5×10^4 to 2.5×10^4 cells/well (depending on the cell line) and left to adhere overnight at 37 °C. Cells were then incubated with the Cu-complexes and respective ligands at different concentrations (0–50 μM) during 48 h at 37 °C. All tested compounds were first solubilized in DMSO (20 mM stock solution) and then diluted in culture medium for the assay, with the percentage of organic solvent in the final solution never exceeding 0.1%. The stock solutions of **CuGTSMpip** and **CuGTSMmor** were prepared in DMSO, similarly to CuGTSM, that was more difficult to solubilize. After incubation, the medium was removed, the cells were washed with PBS and then incubated with MTT (200 μL of 0.5 mg/mL solution in MEM without phenol red) for 3 h at 37 °C. The MTT solution was then removed and the insoluble blue formazan crystals formed were dissolved in DMSO. The absorbance of this colored solution was measured at 570 nm in a plate spectrophotometer (Power Wave Xs; Bio-Tek). Each test was performed with at least six replicates. The results were expressed as the percentage of the surviving cells in relation to the control, which was incubated without any compound. IC_{50} values were determined using Graph Pad Prism.

Table 3. Physicochemical properties of ^{64}Cu(II) complexes: octanol-water partition coefficients (log $D_{7.4}$) and chromatography data (R_t in HPLC).

Complex	log $D_{7.4}$ (±SD)	HPLC [R_t, min][a] ^{nat}Cu	^{64}Cu
^{64}CuGTSM	1.08 (0.19)	12.07	12.84
^{64}CuGTSMpip	0.32 (0.03)	10.87	11.13
^{64}CuGTSMmor	0.89 (0.14)	9.28	9.35

[a] HPLC method I.

Temperature-dependent cellular uptake

Temperature- and time-dependent accumulation of ^{64}Cu-complexes was assessed in PC3 and MCF-7 cancer cells. Cells were seeded at a density of $1.5–2\times10^5$ cells/well in a 24-well tissue culture plate and allowed to attach overnight. On the day of the experiment, the cells were incubated at 37 °C or 4 °C, for a period of 5 min to 4 h with about 7.4 kBq (≈200 K cpm) of ^{64}Cu-complexes in 0.5 mL of assay medium (MEM with 25 mM HEPES and 0.2% BSA). Incubation was terminated by removing unbound ^{64}Cu-complex and by washing cells with ice-cold PBS with 0.2% BSA. Then, cells were lysed by 10 min incubation with 1 NaOH at 37 °C and the activity of lysates was measured using a gamma counter (LB 2111, Berthold). The percentage of cell-associated radioactivity as a proportion to the total applied radioactivity was calculated and represented as a function of incubation time, and per million cells. Uptake studies were carried out using at least four wells for each time point and data are presented as the average ± SEM.

Cellular retention

The cellular retention of the internalized ^{64}Cu-complexes was determined in PC3 cells, previously seeded in 24-well tissue culture plates, as described before for the cellular uptake assays. Cells were incubated for 2 h 30, at 37 °C, with about 7.4 kBq (≈200 K cpm) of ^{64}Cu-complexes in 0.5 mL of assay medium and washed with cold PBS with BSA 0.2%. Then, the radioactivity released into the culture media (0.5 mL) at 37 °C was monitored during a 24 h incubation period. At different time points, the culture medium was collected, and the cells were lysed with 1 M NaOH (0.5 mL). The activity in both medium (released activity) and lysates (retained activity) was counted using a gamma counter (LB 2111, Berthold) and the percentage of cellular retention calculated and expressed as a function of incubation time. The assay was carried out using at least four wells for each time point.

Modulation of cellular uptake Studies with haloperidol

PC3 and DU145 prostate cancer cells with different levels of expression of σ1-receptors were seeded at a density of $1.5–2\times10^5$ cells/well in a 24-well tissue culture plate and allowed to attach overnight. Then, the cells were incubated at 37 °C, for a period of 5 min to 4 h, with about 7.4 kBq (≈200 K cpm) of ^{64}Cu-complexes in 0.5 mL of assay medium. The blocking studies of σ1 receptors were performed in both cell lines with a 10 min pre-incubation with different concentrations of haloperidol followed by 0.5 and 2 h incubation with the ^{64}Cu-complexes. The assay was terminated as described above and the percentage of cell-associated radioactivity related to the total applied radioactivity represented as a function of incubation time, and per million cells. Uptake studies were carried out using at least four wells for each time point and data are presented as the average ± SEM.

Studies with tamoxifen

PC3 cells were seeded in a 24-well tissue culture plate (1.5×10^5 cells/well) and allowed to attach overnight. The cells were pre-incubated at 37 °C, with tamoxifen (TMX: 10^{-6}, 10^{-5} and 10^{-4} M) during 30 min and then incubated with about 7.4 kBq ($\approx$200000 cpm) of ^{64}Cu-complexes in 0.5 mL of assay medium, for 30, 60 and 180 min. The assay was terminated as described above and the percentage of cell-associated radioactivity related to the total applied radioactivity represented as a function of incubation time. Uptake studies were carried out using at least four wells for each time point and data are presented as the average ± SEM.

Confocal microscopy lysosomal assay

PC3 cells were seeded at a density of 2.5×10^5 cells on a coverslip placed in a 6-wells plate and allowed to attach overnight. Then, the medium was replaced either with medium with DMSO (as a negative vehicle control) or medium with the different compounds at a concentration equivalent to their IC_{50} at 48 h. After incubation, 75 nM Lyso-Tracker™ Red DND-99 (Invitrogen) and Hoechst 33342 (1 μg/mL; Invitrogen) were added simultaneously and the cells were incubated for 30 min at 37 °C. Samples were then washed twice, mounted on Hank's Balanced Salt Solution (HBSS) onto a glass slide, and sealed with nail polish. Fluorescence was visualized on a confocal microscope (Zeiss LSM 710) using a 4× immersion oil objective.

Acknowledgements

This work was supported by Fundação para a Ciência e a Tecnologia (FCT), Portugal through the Research Unit grant to C²TN (UID/Multi/04349/2019), fellowship SFRH/BPD/80758/2011 to E. Palma and projects PTDC/MED-QUI/1554/2020 to AP and PTDC/BTM-TEC/29256/2017, co-funded by Lisboa2020 – EU FEDER to FM. The authors also thank FCT for financial support through RNEM – Portuguese Mass Spectrometry Network. We thank Professor Carmen Jerónimo from the Cancer Biology & Epigenetics Group, Portuguese Institute of Oncology, Porto (Portugal) for the generous gift of the cell lines used in this study. The authors would also like to thank Pedro Reis from C²TN for the elemental analyses.

Conflict of Interest

The authors declare no conflict of interest.

Keywords: Antitumor agents · Bis(thiosemicarbazone)s · Cellular studies · Copper · Metallodrugs

[1] a) C. Santini, M. Pellei, V. Gandin, M. Porchia, F. Tisato, C. Marzano, *Chem. Rev.* **2014**, *114*, 815–862; b) C. Shuhong, C. Xiahui, C. Ligen, C. Jingwen, *Anti-Cancer Agents Med. Chem.* **2016**, *16*, 973–991; c) A. E. Stacy, D. Palanimuthu, P. V. Bernhardt, D. S. Kalinowski, P. J. Jansson, D. R. Richardson, *J. Med. Chem.* **2016**, *59*, 4965–4984; d) K. C. Park, L. Fouani, P. J. Jansson, D. Wooi, S. Sahni, D. J. R. Lane, D. Palanimuthu, H. C. Lok, Z. Kovacevic, M. L. H. Huang, D. S. Kalinowski, D. R. Richardson, *Metallomics* **2016**, *8*, 874–886.

[2] F. Cortezon-Tamarit, S. Sarpaki, D. G. Calatayud, V. Mirabello, S. I. Pascu, *Chem. Rec.* **2016**, *16*, 1380–1397.

[3] a) F. Dehdashti, M. A. Mintun, J. S. Lewis, J. Bradley, R. Govindan, R. Laforest, M. J. Welch, B. A. Siegel, *Eur. J. Nucl. Med. Mol. Imaging* **2003**, *30*, 844–850; b) J. P. Holland, J. S. Lewis, F. Dehdashti, *Q J. Nucl Med Mol Imaging* **2009**, *53*, 193–200; c) S. Carlin, J. L. Humm, *J. Nucl. Med.* **2012**, *53*, 1171–1174.

[4] a) P. J. Jansson, D. S. Kalinowski, D. J. R. Lane, Z. Kovacevic, N. A. Seebacher, L. Fouani, S. Sahni, A. M. Merlot, D. R. Richardson, *Pharmacol. Res.* **2015**, *100*, 255–260; b) Z.-L. Guo, D. R. Richardson, D. S. Kalinowski, Z. Kovacevic, K. C. Tan-Un, G. C.-F. Chan, *J. Hemat. Oncol.* **2016**, *9*, 98; c) A. E. Stacy, D. Palanimuthu, P. V. Bernhardt, D. S. Kalinowski, P. J. Jansson, D. R. Richardson, *J. Med. Chem.* **2016**, *59*, 8601–8620; d) E. M. Gutierrez, N. A. Seebacher, L. Arzuman, Z. Kovacevic, D. J. Lane, V. Richardson, *Biochim. Biophys. Acta* **2016**, *1863*; e) C. Stefani, Z. Al-Eisawi, P. J. Jansson, D. S. Kalinowski, D. R. Richardson, *J. Inorg. Biochem.* **2015**, *152*, 20–37.

[5] E. Palma, F. Mendes, G. R. Morais, I. Rodrigues, I. C. Santos, M. P. Campello, P. Raposinho, I. Correia, S. Gama, D. Belo, V. Alves, A. J. Abrunhosa, I. Santos, A. Paulo, *J. Inorg. Biochem.* **2017**, *167*, 68–79.

[6] a) J. Fan, Z. Han, Y. Kang, X. Peng, *Sci. Rep.* **2016**, *6*, 19562; b) S. Daum, M. S. V. Reshetnikov, M. Sisa, T. Dumych, M. D. Lootsik, R. Bilyy, E. Bila, C. Janko, C. Alexiou, M. Herrmann, L. Sellner, A. Mokhir, *Angew. Chem.* **2017**, *56*, 15545–15549; c) B. M. Paterson, C. Cullinane, P. J. Crouch, A. R. White, K. J. Barnham, P. D. Roselt, W. Noonan, D. Binns, R. J. Hicks, P. S. Donnelly, *Inorg. Chem.* **2019**, *58*, 4540–4552.

[7] E. Palma, H. M. Botelho, G. R. Morais, I. Rodrigues, I. C. Santos, M. P. C. Campello, P. Raposinho, A. Belchior, S. S. Gomes, M. F. Araujo, I. Correia, N. Ribeiro, S. Gama, F. Mendes, A. Paulo, *J. Biol. Inorg. Chem.* **2019**, *24*, 71–89.

[8] a) K. Y. Djoko, P. S. Donnelly, A. G. McEwan, *Metallomics* **2014**, *6*, 2250–2259; b) P. J. Crouch, L. W. Hung, P. A. Adlard, M. Cortes, V. Lal, G. Filiz, K. A. Perez, M. Nurjono, A. Caragounis, T. Du, K. Laughton, I. Volitakis, A. I. Bush, Q. X. Li, C. L. Masters, R. Cappai, R. A. Cherny, P. S. Donnelly, A. R. White, K. J. Barnham, *PNAS* **2009**, *106*, 381–386; c) P. S. Donnelly, J. R. Liddell, S. Lim, B. M. Paterson, M. A. Cater, M. S. Savva, A. I. Mot, J. L. James, I. A. Trounce, A. R. White, P. J. Crouch, *PNAS* **2012**, *109*, 47–52.

[9] a) M. A. Cater, H. B. Pearson, K. Wolyniec, P. Klaver, M. Bilandzic, B. M. Paterson, A. I. Bush, P. O. Humbert, S. La Fontaine, P. S. Donnelly, Y. Haupt, *ACS Chem. Biol.* **2013**, *8*, 1621–1631; b) D. Palanimuthu, S. V. Shinde, K. Somasundaram, A. G. Samuelson, *J. Med. Chem.* **2013**, *56*, 722–734.

[10] D. Denoyer, H. B. Pearson, S. A. S. Clatworthy, Z. M. Smith, P. S. Francis, R. M. Llanos, I. Volitakis, W. A. Phillips, P. M. Meggyesy, S. Masaldan, M. A. Cater, *Oncotarget* **2016**, *7*.

[11] T. A. Su, D. S. Shihadih, W. Cao, T. C. Detomasi, M. C. Heffern, S. Jia, A. Stahl, C. J. Chang, *J. Am. Chem. Soc.* **2018**, *140*, 13764–13774.

[12] a) M. Wehbe, A. W. Y. Leung, M. J. Abrams, C. Orvig, M. B. Bally, *Dalton Trans.* **2017**, *46*, 10758–10773; b) K. Y. Djoko, M. M. Goytia, P. S. Donnelly, M. A. Schembri, W. M. Shafer, A. G. McEwan, *Antimicrob. Agents Chemother.* **2015**, *59*, 6444–6453.

[13] K. Ohui, E. Afanasenko, F. Bacher, R. L. X. Ting, A. Zafar, N. Blanco-Cabra, E. Torrents, O. Dömötör, N. V. May, D. Darvasiova, É. A. Enyedy, A. Popović-Bijelić, J. Reynisson, P. Rapta, M. V. Babak, G. Pastorin, V. B. Arion, *J. Med. Chem.* **2019**, *62*, 512–530.

[14] E. Vitaku, D. T. Smith, J. T. Njardarson, *J. Med. Chem.* **2014**, *57*, 10257–10274.

[15] J. L. Dearling, J. S. Lewis, G. E. Mullen, M. J. Welch, P. J. Blower, *J. Biol. Inorg. Chem.* **2002**, *7*, 249–259.

[16] G. Wuitschik, E. M. Carreira, B. Wagner, H. Fischer, I. Parrilla, F. Schuler, M. Rogers-Evans, K. Müller, *J. Med. Chem.* **2010**, *53*, 3227–3246.

[17] B. M. Paterson, J. A. Karas, D. B. Scanlon, J. M. White, P. S. Donnelly, *Inorg. Chem.* **2010**, *49*, 1884–1893.

[18] R. Anjum, D. Palanimuthu, D. S. Kalinowski, W. Lewis, K. C. Park, Z. Kovacevic, I. U. Khan, D. R. Richardson, *Inorg. Chem.* **2019**, *58*, 13709–13723.

[19] K. Sugano, M. Kansy, P. Artursson, A. Avdeef, S. Bendels, L. Di, G. F. Ecker, B. Faller, H. Fischer, G. Gerebtzoff, H. Lennernaes, F. Senner, *Nat. Rev. Drug Discovery* **2010**, *9*, 597–614.

[20] A. van Waarde, A. A. Rybczynska, N. K. Ramakrishnan, K. Ishiwata, P. H. Elsinga, R. A. J. O. Dierckx, *Biochim. Biophys. Acta* **2015**, *1848*, 2703–2714.

[21] C. S. John, B. J. Vilner, B. C. Geyer, T. Moody, W. D. Bowen, *Cancer Res.* **1999**, *59*, 4578–4583.

[22] C. de Duve, T. de Barsy, B. Poole, A. Trouet, P. Tulkens, F. Van Hoof, *Biochem. Pharmacol.* **1974**, *23*, 2495–2531.

[23] a) A. C. MacIntyre, D. J. Cutler, *Biopharm. Drug Dispos.* **1988**, *9*, 513–526; b) E. Agostinelli, N. Seiler, *Int. J. Oncol.* **2007**, *31*, 473–484; c) N. Altan, Y. Chen, M. Schindler, S. M. Simon, *PNAS* **1999**, *96*, 4432–4437.
[24] P. A. Bokhan, N. V. Fateev, T. V. Malin, I. V. Osinnykh, D. E. Zakrevsky, K. S. Zhuravlev, *J. Lumin.* **2018**, *203*, 127–134.
[25] P. Kannan, C. John, S. S. Zoghbi, C. Halldin, M. M. Gottesman, R. B. Innis, M. D. Hall, *Clin. Pharmacol. Ther.* **2009**, *86*, 368–377.
[26] A. R. Cowley, J. Davis, J. R. Dilworth, P. S. Donnelly, R. Dobson, A. Nightingale, J. M. Peach, B. Shore, D. Kerr, L. Seymour, *Chem. Commun.* **2005**, 845–847.
[27] T. J. Hoffman, W. A. Volkert, D. E. Troutner, R. A. Holmes, *Int. J. Appl. Radiat. Isot.* **1984**, *35*, 223–225.

Manuscript received: February 25, 2021
Revised manuscript received: February 25, 2021
Accepted manuscript online: February 26, 2021